Metal Chelates with Biological Activity. Part 4. Solution Properties of Iron(III)–Histidinehydroxamic acid

DAVID A. BROWN and B. S. SEKHON*

Department of Chemistry, University College, Belfield, Dublin 4, Ireland

Received July 5, 1983

Introduction

In this paper, we discuss the application of *in vitro* chemical criteria previously suggested as suitable indicators of biological activity [1] to the chelate, ferric histidinehydroxamate. As in previous papers, the aim is to design a metal chelate as a suitable source of trace elements essential in animal nutrition with iron as trace element and in particular with its complexes with histidinehydroxamic acid.

Experimental Section

Histidinehydroxamic acid was synthesized following the published procedure [2] and its purity was checked potentiometrically. Distilled deionized water was used throughout and all titrations were carried out under an atmosphere of purified argon. The base used for pH measurement was carbonate free sodium hydroxide (2.9656 *M*) and was standardized by using oven-dried potassium hydrogen phthalate. Stock solutions of ferric chloride were prepared from 'Titrosol' $FeCl_3$ (Merck) solution, and 'Titrosol' HCl stock solution was used. All other reagents were of analytical grade.

Potentiometric titrations were performed using a Radiometer (Copenhagen) automatic titrations apparatus; pH meter readings were recorded on a Digital PHM64. Small amounts of base were added with the use of an ABU13 autoburette (volume 0.25 ml). Titrations were recorded graphically using an TTT60 automatic titrator and an automatic recorder REC 61 Servograph. The 50 ml solutions employed were thermostatted to 25 ± 0.1 °C using a water circulation pump. The electrode pair consisted of a Radiometer G2040C glass electrode and a K4050 KCl electrode. Nuclear magnetic resonance spectra were obtained on a Perkin-Elmer R12B instrument. The method of Evans [3] was used to determine the magnetic moments of solutions in the pH range 2.0–10.5. Ferric citrate polymer was prepared as described earlier [4]. The depolymerization reaction was followed by monitoring the rate of appearance of the Fe^{3+} complex with histidine–hydroxamic acid at 515 nm. Absorption spectra were obtained on a Perkin-Elmer 124 spectrophotometer at 25 °C. Infrared spectra were recorded with a Perkin-Elmer 283B infrared spectrophotometer. The concentrations of ligand solutions were 0.1–0.2 *M* in 99.8% D_2O as solvent. The pD of the solution was varied by the addition of 30% NaOD and 20% DCl in D_2O (99.8%). The conversion from pH to pD was made using the equation pD = pH + 0.40.

Human transferrin approximately 98% iron free was obtained from Sigma Chemical Co., London. Iron(III) chelate was freshly prepared. The ratio of ligand to Fe(III) was 10:1. Dilution of the stock solution was also done immediately prior to kinetic runs in CO^{-}_3/HCO^{-}_3 buffer (pH = 7.4). Kinetics of the iron-transfer reactions between $Fe(HHA)_2$ and apotransferrin were followed at 25 °C on a UV–visible spectrophotometer. The spectra showed a biphasic reaction by changes in the absorption at 585 nm with a complex concentration of 10^{-3} *M* and protein concentration of 5×10^{-3} *M* before half dilution on mixing. After mixing, there was a rapid decrease in absorbance followed by a slower first order decrease in absorbance at 585 nm.

Methods

Sarkar–Kruck Method. A method introduced by Osterberg [5] for the measurement of free ligand concentration during the formation of metal complexes has been extended by Sarkar and Kruck [6] to include the measurement of free-metal concentration. The calculations have been improved by the introduction of computer-based numerical procedures. Full details of the method are given in reference [6].

*Present address: Department of Biochemistry, Punjab Agricultural University, Ludhiana 141004, India.

0020-1693/84/$3.00

Irving–Rossotti Method. The above standard technique [7] was used to determine both proton–ligand and metal–ligand stability constants.

Potentiometric titrations were carried out on a series of solutions (50 ml total volume) 0.15 *M* in NaCl and sufficient HCl to bring the starting pH close to 2.0. In the proton–ligand system, titration curves were obtained at various initial histidinehydroxamic acid concentrations (C_A) at 1.8, 2.88, 3.6 and 5.4 m*M* respectively. In the determination of metal–ligand constants, the concentration of HCl was kept constant (2.4 m*M*) and the two sets of curves were obtained. The first set was at constant ligand concentration (C_A = 3.6 m*M*) with variation of metal concentration (C_M = 0.2, 0.4 and 0.8 m*M*), the second set was at constant metal concentration (C_M = 0.4 m*M*) with variation of ligand concentrations (C_A = 1.8, 3.6 and 5.4 m*M*). The resulting formation constants are given in Table I.

TABLE I. Logarithmic Stability Constants (log β_{par} and log K_n) of Complex species $M_pH_qA_r$ (M = Fe^{3+}, A = Histidinehydroxamic acid) in 0.15 *M* NaCl at 25 °C.

p	q	r	Sarkar–Kruck Method log β_{pqr}	Irving-Rossotti Method log K_n
0	3	1	9.11	9.20
0	2	1	7.22	7.26
0	1	1	5.40	5.51
1	2	1	22.148	
1	1	1	18.070	
1	0	1	13.389	13.425
1	2	2	31.372	
1	1	2	25.885	
1	0	2	18.984	19.05
1	0	3	21.606	22.11
1	−1	3	12.441	

A maximum number of three protons can be liberated from the ligand in the protonated form (I) on titration with strong base in the pH range 2.0–11.0.

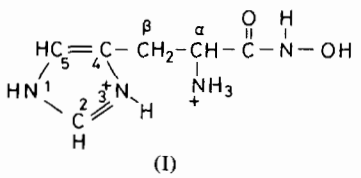

(I)

The proton liberation $\delta H^+/\delta C_A$ as a function of pH was obtained by processing the titration curves of ligands at 1.8, 3.6 and 5.6 m*M* using the PLOT II program. Protonation constants β_{011}, β_{012} and β_{013} of the species HA, H_2A and H_3A were obtained from analysis of curves using the LEASK II program. Refined values of the protonation constants are in good agreement with those obtained by Irving–Rossotti method (Table I).

The concentrations of unbound metal p*M* as a function of pH at C_A = 3.6 m*M* were obtained by digitizing the titration data from the ligand variation titration curves and processing the data by PLOT II program. The concentration of unbound ligand as a function of pH at C_M = 4 m*M* were similarly obtained from PLOT II analysis of metal variation titration curves. Values of $\delta H^+/\delta C_A$ and $\delta H^+/\delta C_M$ as a function of pH were also obtained.

The presence of likely metal–proton–histidinehydroxamic acid species were tested for by using the following values: p = 1; q = −3, −2, −1, 0, 1, 2, 3 and r = 1, 2 and 3. To select the existing species in the system, the above values for p, q and r together with the pM and pA values generated in the PLOT II analysis, were used as an imput for the GUESS program. Processing with LEASK II to determine β_{pqr} values showed that the species MH_2A, MHA, MA, MA_2H_2, MA_2H, MA_2, MA_3 and MA_3H_{-1} were required to give a minimum error solution.

Results and Discussion

State of Aggregation

The magnetic moments of solutions of ferric histidinehydroxamic acid were determined as a function of pH for various [ligand]/[metal] ratios. For [ligand]/[metal] ratios of 5:1, the magnetic moments of solutions slowly changed with time and for [ligand]/[metal] ratios of 10:1, the change in moments was very slow with time. The magnetic moments of ferric histidinehydroxamic acid solutions are plotted as a function of pH for [ligand]/[metal] ratios of 20:1 (Fig. 1). In this case, no change in moment was observed with time and no reduction in moment occurred until pH ⩾ 9.5. On the assumption that reduction in magnetic moment implies metal–

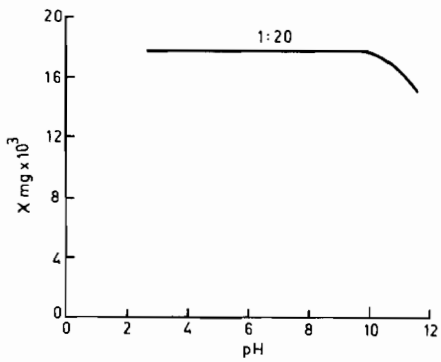

Fig. 1. Dependence of $\chi_m \times 10^{-3}$ (molar susceptibility) of Fe(III) in the Fe(III)/Histidinehydroxamic acid system as a function of pH, $C_M = 2 \times 10^{-3}$ *M*; $C_A = 4 \times 10^{-2}$ *M*.

metal interaction as in a polymeric species, it follows that for [ligand]/[metal] ratio $\geqslant$ 20:1, the chelate is present as a monomer.

Species Distribution

The species distribution for a metal concentration, $C_M = 4 \times 10^{-4}$ *M* and ligand concentration $C_A = 3.6 \times 10^{-3}$ *M* is given in Fig. 2 and the stability

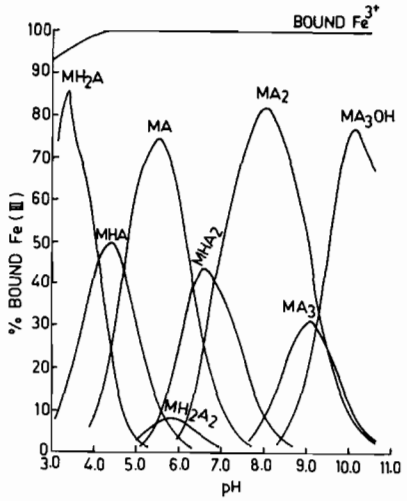

Fig. 2. Species distributions in the Fe(III)/Histidinehydroxamic acid system as a function of pH, $C_M = 4 \times 10^{-4}$ *M*; $C_A = 3.6 \times 10^{-3}$ *M*.

constants of the various protonated species in Table I. Histidinehydroxamic acid has three titratable protons in the studied pH range 2.0–10.5 which can be attributed to the imidazole, the OH group of the NHOH and the NH_3^+ group and the pK_a values are reported in Table I. The presence of the α-amino group in histidinehydroxamic acid increases the acidic character of the OH group in comparison with that of acetohydroxamic acid (pK^H = 9.342 [4]). Similarly, comparison of the pK_3^H for histidinehydroxamic acid with that of histidine pK_3^H = 6.06 [8] shows that substitution of an NHOH group for the OH group of a carboxyl lowers the pK_a in accord with the electron-withdrawing character of the NHOH group. Finally, comparison of pK_2^H for histidinehydroxamic acid with pK_2^H = 7.52 for glycinehydroxamic acid [9] shows that the presence of the imidazole ring lowers the pK_a of the OH of the NHOH group.

In the presence of Fe^{3+}, the proton liberation data (Fig. 3) shows that complexation begins at low pH values (<3.0). The displacement of one proton at pH 3.4 presumably gives an MH_2A species and at pH 4.4, the predominant species is MHA corresponding to the displacement of two protons. At pH 5.5, the proton displacement value rises to about 2.5 and can be attributed to the formation of the MA species when the imidazole group is about 50% ionized. The displacement of 2.5 protons can thus be attributed

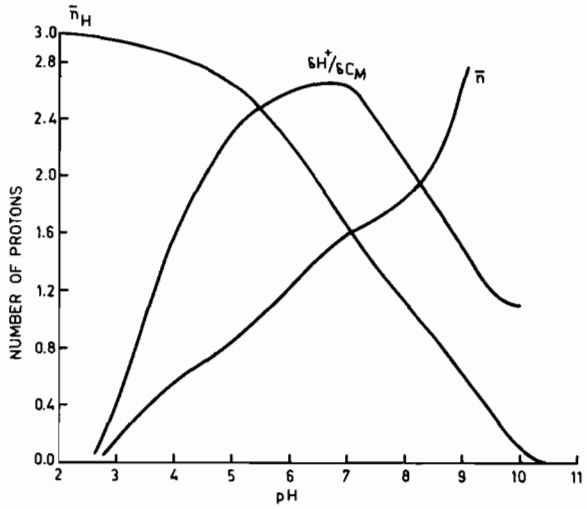

Fig. 3. Molar proton liberation $\delta H^+/\delta C_M$ and its relationship to $\bar{n}_H$ and $\bar{n}$.

to those from the imidazole, the OH group of NHOH and the NH_3^+ group respectively. On raising the pH further, MH_2A_2, MHA_2, MA_2, MA_3 and MA_3OH species form. At pH 8.0, approximately two protons per mole of Fe^{3+} are liberated and the predominant species is MA_2. At this pH, the hydroxamic acid group is about completely ionized whereas the NH_3^+ group is largely unionized; therefore the displacement of two protons must be due to complexation of the two NH_3^+ groups. In the physiological pH range (6.7–7.3), MA_2H and MA_2 account for over 90% of the species present and there is no evidence for any polymeric species. Above pH 8.3, MA_3 and MA_3H_{-1} species are obtained. Increasing the pH beyond the amino group pK_a value (pH = 9.1) results in a decrease of the proton liberation $\delta H^+/\delta C_M$, implicating the amino group in Fe^{3+} co-ordination. The value of $\delta H^+/\delta C_M \cong 1.5$ at pH 9.1 means that more than two amino groups are involved in complexation. Above pH 9.5, one hydroxyl species was detected. Finally, it is gratifying that the stability constants calculated by both methods agree closely (Table I) but as stressed previously the method of Sarkar and Kruck possesses the great advantage of giving an accurate species distribution as a function of pH.

Electronic spectra/pH Profile

The visible absorption spectra of mixed metal/ligand solutions (C_M = 0.2 m*M* and C_A = 3.6 m*M*) were recorded in the pH range 3.0 to 11.0. As shown in Fig. 4, the spectra in the pH range 3.5 to 8.0, consist of two absorption bands at 585 nm and 520–510 nm. The maximum purple colour is observed between pH 6 and 7 and the absorption bands at 585 and 515 nm have molar absorptivities of 1850 and 2000 M^{-1} cm^{-1} respectively. With increasing pH, λ_{max} progressively shifts from 520 to 510 nm. In

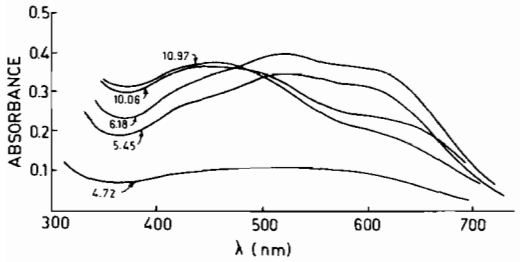

Fig. 4. Visible spectra of Fe(III)/Histidinehydroxamic acid as a function of pH, $C_M = 2 \times 10^{-4}$ *M*; $C_A = 3.6 \times 10^{-3}$ *M*.

the pH range 6–7, the predominant species are MHA_2 and the stepwise association of free ligand about the metal ion is virtually complete to give MA_2. At pH 9, the colour of the solution changes to purple brown and λ_{max} at 515 nm shifts to 470 nm. As the pH is increased to 11, λ_{max} progressively shifts from 470 nm to 455 nm ($\epsilon \sim 1850\ M^{-1}\ cm^{-1}$). At pH 9, when the predominant species is MA_3, the appearance of a new absorption band suggests a change in ligand composition around the metal ion. The Fe(III)/glycinehydroxamic acid system gave λ_{max} at 470 nm at low pH values but with increase in pH, there was a shift of λ_{max} towards shorter wavelengths [9]. The pH dependence of Fe(III)/histidinehydroxamic acid solution thus differs from that of Fe(III)/glycinehydroxamic acid solution in the pH range 3 to 8 but is similar in the pH region 9–11. Glycinehydroxamic acid coordinates to Fe^{3+} via the α-amino nitrogen and the hydroxyl oxygen of the NHOH group [9] suggesting similar coordination in the MA_3 species of the present system.

Infrared Spectra

The infrared spectra of D_2O solutions of histidinehydroxamic acid are given in Table II. At low pD values important absorption bands occur at 1680 and 1450 cm^{-1} but on increasing the pD to 6.4 and 8.3, the band at 1680 cm^{-1} is replaced by a band at 1670 and 1645 cm^{-1} respectively. At a high pD value of 11.6, bands at 1615, 1560 and 1445 cm^{-1} are observed. The band at 1680 cm^{-1} is assigned to an amide I mode (amide of COND, mainly CO stretching) and the inductive effect of the adjacent $\overset{+}{N}D_3$ group is responsible for the shifts of absorption to higher frequency compared with the value in acetohydroxamic acid [10]. In the completely deprotonated ligand, the band due to the amide I mode is observed at ~1615 cm^{-1} and also an amide II band appears at 1560 cm^{-1}. The amide II band at ~1570 cm^{-1} (contribution from the in-plane deformation vibration of N–H and C–N stretching vibrations 60% of δ(NH) and 40% of ν(C–N)) and the in-plane deformation vibrations of N–H at 1440–1400 cm^{-1} have been assigned previously [11, 12]. The spectra of 1:1 Fe–histidinehydroxamic acid solutions and the main absorption bands are given in Table II. At low pD values, the spectra of Fe–histidinehydroxamic acid solutions are similar to those of the free ligand. At pD 3.9, two absorption bands with maxima at 1680 and 1615 cm^{-1} are observed. The 1615 cm^{-1} band is new and must come from metal complex formation. The main species at this pD is MH_2A. Of the four main bands at pD 5.3 and 6.3 (1620, 1560, 1510 and 1445 cm^{-1}) the 1510 cm^{-1} band arises from the stretching mode of coordinated imidazole and the similar band is observed at 1500 cm^{-1} for the Cu(II)/histidine system [13]. The free imidazole ring absorption is not observed in the ligand spectra due to the very strong absorption band at 1450 cm^{-1} due to C–N and N–H vibrations. The bands at 1620 and 1560 cm^{-1} observed on complex formation are similar to bands due to the completely dissociated ligand and in this pD range, the main species is MA. At higher pD values precipitation

TABLE II. Infrared Spectra of Histidinehydroxamic acid on Fe^{3+} Complexes, in D_2O (cm^{-1}).

Histidinehydroxamic acid				
pD 1.2	pD 6.4	pD 8.3	pD 11.6	Assignment
1680	1670	1645	1615	Amide I band (main contribution CO)
1450	1450	1445	1445	Amide II band
	1560(sh)	1560(sh)	1560	Amide II band
Histidinehydroxamic acid/Fe^{3+} (1/1) Complexes				
pD 2	pD 3.9	pD 5.3	pD 6.3	Assignment
1680	1680	1620	1620	Amide I band
	1615			
1450	1445	1445	1445	Amide band
1560(sh)	1560(sh)	1560	1560	Amide II band
		1510	1510	Ring Str. (Imidazol)

occurs and so no further solution infrared studies were possible. It is suggested therefore that coordination of Fe(III) occurs by the imidazole N(3), the nitrogen of the amino group and oxygen atom of the hydroxamate group.

Proton Magnetic Resonance Spectra

The pD dependence of the ^{1}H NMR chemical shifts of the α and β protons and those at positions 2 and 5 of the imidazole ring are shown in Fig. 5. The proton group closest to the ionization site is expected to show the largest upfield shift on ionization. Thus the C_2 proton of the imidazole moiety shows the largest upfield shift in the pD range 4.5 to 7.0 when proton ionization occurs from the imidazole ring. The α-CH proton of the alanine moiety shows the largest upfield shift in the pD range 6.5 to 10.0 where proton ionization from both the OH of the NHOH group and $\overset{+}{N}H_3$ group occurs.

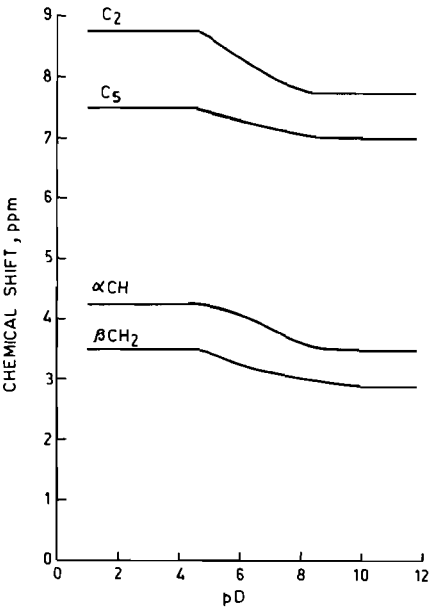

Fig. 5. pD dependence of chemical shift of C_2 and C_5 protons of imidazole ring, αCH and βCH_2 protons of Histidinehydroxamic acid.

The ^{1}H NMR spectra of histidinehydroxamic acid in the presence of small amounts of Fe(III) (1:50) show distinctive changes. The signal corresponding to the carbon(2) imidazole proton becomes progressively broader from pD 4.6 indicating interaction of Fe(III) with the N(3) atom of the imidazole ring. In contrast, the signal for the α-CH proton remains broadened in the whole pD region. Since the β-CH_2 group in histidinehydroxamic acid is situated between the two coordination sites, it should be most affected by the presence of the paramagnetic ferric ion. The progressive changes of the β-CH_2 proton signals with varying pD give further support for the coordination of both the N(3) of imidazole ring and the $\overset{+}{N}H_3$ group. At the low values of pD the broadening of the imidazole, the β-CH_2 and the α-CH proton signals is large. However, at pD 10.3, the signals due to the C(2) imidazole proton and β-CH_2 sharpen leaving the α-CH proton signal unaffected indicating that at high pD values, the imidazole ring does not coordinate with Fe^{3+}.

The proposed structures of the major species MA, MA_2 and MA_3 based on the above potentiometric and spectroscopic results are shown in Fig. 6.

Depolymerization Kinetics

The kinetic data for the depolymerization of the ferric citrate polymer are given in Table III. An initial rapid increase in absorbance is followed by a first order increase from which the rate constants were derived. The fraction of total absorbance change due to the initial rapid increase was almost 20% which is in good agreement with the 20% monomer reported previously in the polymer solution [14]. For histidinehydroxamic acid, the rate constants are about ten times those of other iron(III) chelates but smaller than those of acetohydroxamic acid and glycinehydroxamic acid [9].

Kinetics of Iron Transfer to Apotransferrin

As discussed previously [1], the rate of transfer of iron from a chelate to apotransferrin may be a critical factor in determining the efficacy of a given iron chelate as an oral source of iron. In the case of histidinehydroxamic acid it was found that mixing

TABLE III. Depolymerization Kinetics for Fe Citrate (polymeric) + L → FeL + Citrate.

Ligand (L)	Fe citrate/L	$10^5 \cdot$k obsd (s^{-1})	Ref.
NaH_2 citrate	1:50	4.775	[14]
Na_2H_2 EDTA	1:50	3.166	[14]
Na_2H citrate	1:50	1.972	[14]
Acetohydroxamic acid (AHA)	1:100	35.59	[14]
Glycinehydroxamic acid (GHA)	1:100	22.68	[9]
Histidinehydroxamic acid (HHA)	1:50	12.77	present
	1:100	14.66	work

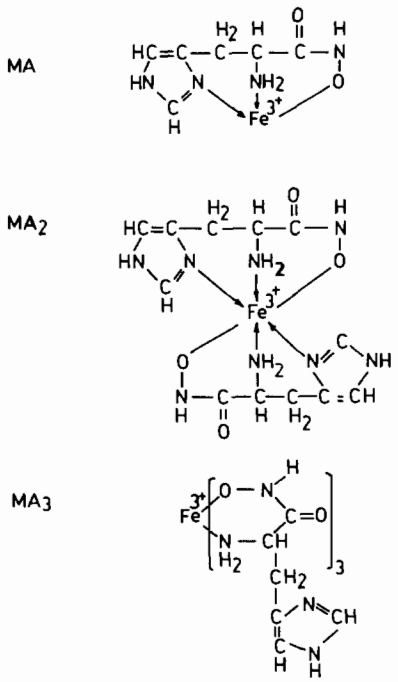

Fig. 6. Proposed structures of various species in the Fe(III)/Histidinehydroxamic acid system.

equal volumes of the chelate solution and apotransferrin solution gave rapid formation of an intermediate (λ_{max} = 490 nm) which is presumably a ternary complex as suggested previously [15]. However, in contrast to aceto- and glycinehydroxamic acids [9], subsequent reaction is slow and can be measured without recourse to stopped-flow techniques. The resulting rate constant is given in Table IV.

TABLE IV. Rates of Fe^{3+} Exchange between Chelates and Apotransferrin.

		Ref.
Fe(EDTA)	0.85×10^{-3} min^{-1}	[16]
Fe cit	2.5×10^{-3} min^{-1}	[16]
Fe(NTA)	5.5×10^{-1} s^{-1}	[15]
Fe(AHA)	1.59×10^{-2} s^{-1}	[4]
Fe(GHA)	1.7×10^{-1} s^{-1}	[9]
Fe(HHA)	3.0×10^{-4} s^{-1}	

Conclusions

The concerted use of several techniques has led to a reasonably full description of the chelation of histidinehydroxamic acid on Fe^{3+}. Our results show that in the major species MA and MA_2 histidinehydroxamic acid coordinates to Fe^{3+} *via* the N(3) of imidazole ring, α-amino nitrogen and the hydroxyl oxygen of the NHOH group. In MA_3, bidentate coordination *via* the α-amino nitrogen and the hydroxamate OH group is suggested. The aqueous solutions contain monomeric species in the pH range 2 to 9.5 and there is no evidence of polymeric species at physiological pH values in the presence of excess ligand. The kinetic criteria show effective depolymerization of ferric citrate polymer and donation of Fe^{3+} by Fe^{3+}–$(HHA)_2$ to apotransferrin but in both cases the rates of reaction are considerably slower than for either tris(acetohydroxamato–)iron(III) or tris(glycinehydroxamato–)iron(III) suggesting that the iron(III) complex of histidinehydroxamic acid will not be as effective an oral source of iron for mammals as either acetohydroxamic acid or glycinehydroxamic acid.

References

1 D. A. Brown and M. V. Chidambaram, 'Iron-Containing Drugs' in 'Metal Ions in Biological Systems', *14*, 125 (1982), Ed. H. Sigel, Marcel Dekker, New York.
2 E. E. Smissman and V. D. Warner, *J. Med. Chem., 15*(6) 681 (1972).
3 D. F. Evans, *J. Chem. Soc.*, 2003 (1959).
4 D. A. Brown, M. V. Chidambaram, J. J. Clarke and D. M. McAleese, *Bioinorg. Chem.*, 225 (1978).
5 R. Osterberg, *Acta Chem. Scand., 15*, 1981 (1961).
6 B. Sarkar and T. P. Kruck, *Canad. J. Chem., 51*, 3541 (1973).
7 H. M. Irving and H. S. Rossotti, *J. Chem. Soc.*, 2904 (1954).
8 T. P. A. Kruck and B. Sarkar, *Canad. J. Chem., 51*, 3549 (1973).
9 D. A. Brown, M. V. Chidambaram and J. D. Glennon, *Inorg. Chem., 19*, 3260 (1980).
10 A. L. Roche, *Ph. D. Thesis, National University of Ireland* (1981).
11 L. J. Bellamy, 'Advances in Infrared Group Frequencies', Wiley, New York (1968).
12 J. C. D. Brand and G. Eglinton, 'Applications of Spectroscopy to Organic Chemistry', (1965).
13 M. Tasumi, 'Infrared and Raman Spectroscopy of Biological Molecules', Ed. Theo M. Theophanides, p. 225–240 (1979).
14 T. G. Spiro, L. Pape and P. Saltman, *J. Am. Chem. Soc., 89*, 5555, 5559 (1967).
15 G. W. Bates and J. Wernicke, *J. Biol. Chem., 246*, 3679 (1971).
16 G. W. Bates, C. Billups and P. Saltman, *J. Biol. Chem., 242*, 2810, 2816 (1967).